Optik 127 (2016) 5065–5069

Contents lists available at ScienceDirect

Optik

journal homepage: www.elsevier.de/ijleo

# Effects of precursor parameters on the optical and electrical properties of AZO nano-composite films

Ümit Özlem Akkaya Arıer[a,*], Bengü Özuğur Uysal[b]

[a] Department of Physics, Mimar Sinan Fine Arts University, Beşiktaş, Istanbul 34349, Turkey
[b] Department of Energy Systems Engineering, Faculty of Engineering and Natural Sciences, Kadir Has University, Fatih, Istanbul 34083, Turkey

ARTICLE INFO

*Article history:*
Received 5 January 2016
Accepted 9 February 2016

*Keywords:*
Optical properties
Nano-composites
Thin films
Surface properties

ABSTRACT

Al doped ZnO (AZO) nano-composite films were synthesized on glass substrates with the sol–gel spin-coating method at the room temperature. The activation energy of AZO nano-composite films was calculated to be 49 kJ/mol for the particles growth. The electrical, structural and optical properties of AZO films were determined by changing ZnO:water and ZnO:Al ratios. ZnO:water and ZnO:Al ratios play an important role in controlling the electrical conductivity of the AZO nano-composite films. The optimum doping ratio of Al was found to be 2% in terms of the lowest resistivity, and above 2% Al-doping concentration, the surface resistivity of AZO nano-composite films starts to increase. The optical highest transmittance of the films of 86% in visible region, and low surface resistivity of 70 Ω/□ can be obtained for the optimum doping ratio of Al.



## 1. Introduction

Al-doped ZnO (AZO) is a very important transparent conducting oxide (TCO) material that has good electrical and optical properties. AZO structures have a number of applications in electronic devices such as a sensor, solar cell and display devices [1,2]. AZO is commonly used in various applications due to its highly visible transparency and good electrical conductivity. Many methods have been used to prepare AZO films such as sol–gel, chemical vapor deposition (CVD), pulsed laser deposition (PLD), and sputtering [3,4] generally in researches. Zinc oxide (ZnO) which is used in various researches is a semiconductor material that has a wide band gap, a wide range resistivity, high mobility and high transparency [2,5]. It is a cheap, non-toxic and chemically stable metal oxide material. Carriers, which act as donors, are formed through the ionization of zinc interstitials and oxygen vacancies to contribute the native intrinsic n-type conductivity behavior. A well-known wide-band gap, wurtzite structured zinc oxide with four-fold tetrahedral coordination lies in the border between ionic and covalent semiconductors. In our early work [6], we found the properties of nanostructured ZnO nano-composite films can be controlled by changing the Dea:water ratio. In order to understand the similar influences of chemical ratios, in this case, we studied the optical and conductivity properties of the AZO films. Generally, Al atoms are doped to ZnO films for the increment conductivity of the films. In recent years, AZO films were studied by many researchers [7–9]. Especially, the activation energy for the AZO dyes have been calculated to be in the range of 51–101 kJ/mol [10–12], and at least 298 kJ/mol for the Al doped ZnO powders [13], but the activation energy of AZO as form of thin film prepared by sol–gel technique has not been reported before. In this study, the important experimental parameters, such as heat-treatment temperature of the nanostructured films or ZnO:Al and ZnO:water ratio of the sol before annealing were varied in order to understand the influences of these parameters on electrical, structural and optical properties. The growth kinetics of films were investigated and the activation energy was calculated. This value was found to be lower than the values reported in the literature. On the other hand, the crystallite size, band gap energy and sheet resistance of single-layer AZO films were investigated. The resistivity of the AZO thin film is also varied by other parameters, such as crystal orientation, defects, electron scattering at the grain boundaries, high annealing temperature, and different medium (pressure) as mentioned before by other authors [14–17]. These factors also affect the resistivity, but controlling the particle size has a crucial importance among them for further applications of semiconducting thin films. Our calculated resistivity values are comparable and enough low to those findings in the literature. As a result, we expect that the incorporation of Al atoms in the place of Zn lead to the generation of free electrons, to decrease the sheet resistivity of AZO films.

* Corresponding author. Tel.: +90 5323434202; fax: +90 212 2611121.
*E-mail address:* oarier@gmail.com (Ü.Ö.A. Arıer).

http://dx.doi.org/10.1016/j.ijleo.2016.02.020
0030-4026/

## 2. Experimental

### 2.1. Preparation of AZO films

AZO thin films were prepared using sol–gel method. The sol was prepared by dissolving zinc acetate dihydrate (ZnAc) in isopropanol, and then, aluminum butoxide was added. A homogeneous and stable sol was prepared by dissolving the zinc acetate in a solution of isopropanol and diethanolamine. First, as a precursor solution of ZnAc:2propanol:Dea:water:Al, a volume ratio of 0.4:4:0.1:0.2: (1, 2, 3, 4%) was used. Second, ZnAc, Al, 2propanol, Dea, Al (% 2) concentrations were held fixed, and crystallite size was controlled only by changing the ZnO:water volume ratio, e.g., to 5, 4, 2.5 and 2. AZO films were prepared on the corning 2947 glass by a spin coater. These samples were heat-treated at 500 °C for 1 h, and in order to calculate the activation energy, the films were annealed at 550, 600, and 650 °C.

### 2.2. Sample characterization

Structural analysis and surface morphology of the resulting films were carried out by X-ray diffraction (XRD-GBC-MMA, Cu-$K\alpha$ radiation), atomic force microscopy (AFM-Shimadzu scanning probe microscope SPM-9500J3), transmission electron microscopy (HR-TEM), and scanning electron microscopy (SEM – Shimadzu scanning probe microscope SPM-9500J3). The optical analysis of films was determined by a spectrophotometer (Perkin Elmer). Four point probe was used to determine the sheet resistivity of films.

## 3. Results and discussion

### 3.1. Structural analysis

XRD patterns of the nanostructured AZO films which were prepared for different ZnO:Al ratios are shown in Fig. 1A. Three well-defined diffraction peaks were identified as {1 0 0}, {0 0 2}, and {1 0 1} planes of hexagonal wurtzite structured (JCPDS: 36-1451) zincoxide [18,19]. The Al phase was not observed in the XRD diffraction patterns due to the low doping concentration of Al and the insufficient heat treatment temperature for the crystallization of Al. The crystallite sizes of the AZO nanostructured films with different ZnO:Al volume ratio of 1, 2, 3, 4% were determined by using the Scherrer equation [20]

$$D = \frac{K\lambda}{B\cos\theta},$$

where $D$ is the diameter of the nanocrystallites, $K$ is a constant (0.89), $\lambda$ is the wavelength of the incident light (for Cu $K\alpha$ radiation $\lambda = 1.54056$ Å), $B$ is the full width at half-maximum (FWHM) of the diffraction line and $\theta$ is the Bragg angle. The crystallite size increases from 1.78 to 7.9 nm; 2.1 to 9.1 nm; 1.95 to 8.5 nm, for the ZnO:Al volume ratio of 4, 3, 2, 1%, respectively. The results suggested that the crystallinity of AZO thin films is decreased with ZnO:Al volume ratio. The XRD patterns of 2 wt% aluminum doped ZnO synthesized with different ZnO:water volume ratios on a glass substrate are shown in Fig. 1B. The diffraction peaks of AZO nanocomposite films were observed at {1 0 0}, {0 0 2}, and {1 0 1}, which belong to hexagonal wurtzite structure, again. The crystallite sizes are calculated for ZnO:water volume ratios: 5; 4; 2.5; 2 from {1 0 0}, {0 0 2}, and {1 0 1}, and the peaks increases from 5.7 to 10.2 nm, 6.8 to 15.2 nm, and 6.3 to 12.3 nm, respectively. The increment of the water ratios supported the agglomeration and then the crystallite size was increased by decreasing the ZnO:water ratio. The water ratio affects the hydrolysis and the nucleation reactions in AZO solution. The hydrolysis rates are low for less water ratio and too much alkoxide in the solvent. The crystallite size of ZnO nanoparticles in AZO films decreased as the volume of water added increased. These clearly demonstrate that water can control the growth of ZnO nanoparticles in AZO films. It was also noted that the more water ratio present in the solution could favor the high crystallinity of the ZnO nanoparticles in AZO nano-composite films. Fig. 1C shows the diffraction patterns of AZO nano-composite films prepared for various heat treatment temperatures. The influence of the heat treatment temperature on the crystallinity of film was investigated. While ZnO:water at 5 and ZnO:Al at 2 ratios were held fixed, crystallite size was increased by the increment of the

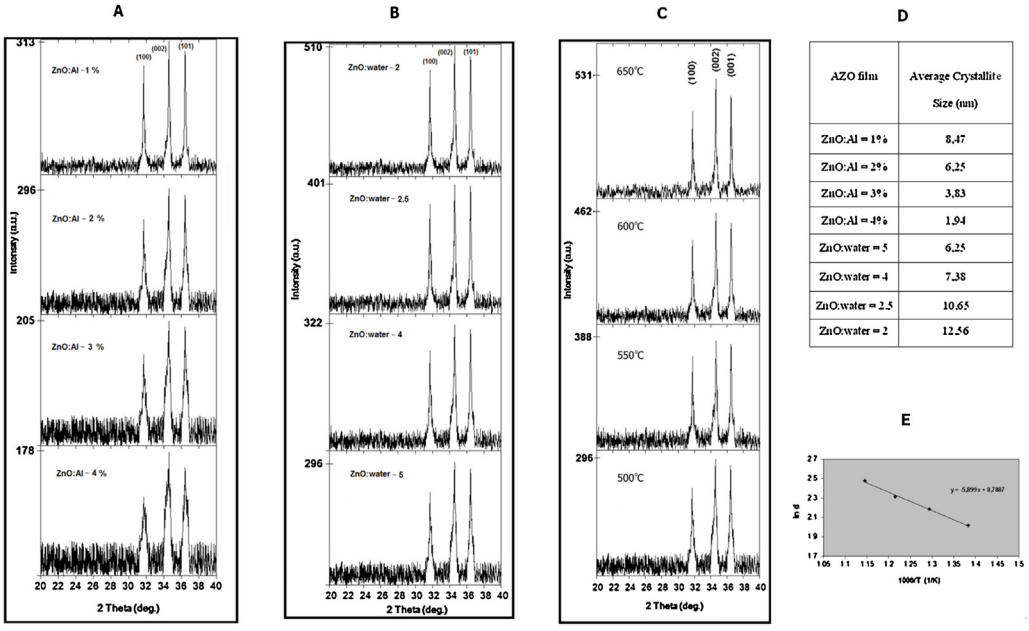


**Fig. 1.** X-ray diffraction patterns of AZO nano films for different (A) ZnO:Al ratios annealed at 500 °C, (B) ZnO:water ratios heat treated at 500 °C, (C) heat treatment temperatures. (D) The calculated average crystallite size of the nanostructured AZO thin films with respect to the varying volume ratio of ZnO:Al and ZnO:water in compositions at annealing temperature of 500 C. (Peak positions in $2\theta$ deg.: 31.72, 34.58, 36.44). (E) Plots of ln $d$ versus 1000/$T$ of AZO nano films (ZnO:water-5, ZnO:Al-2%).

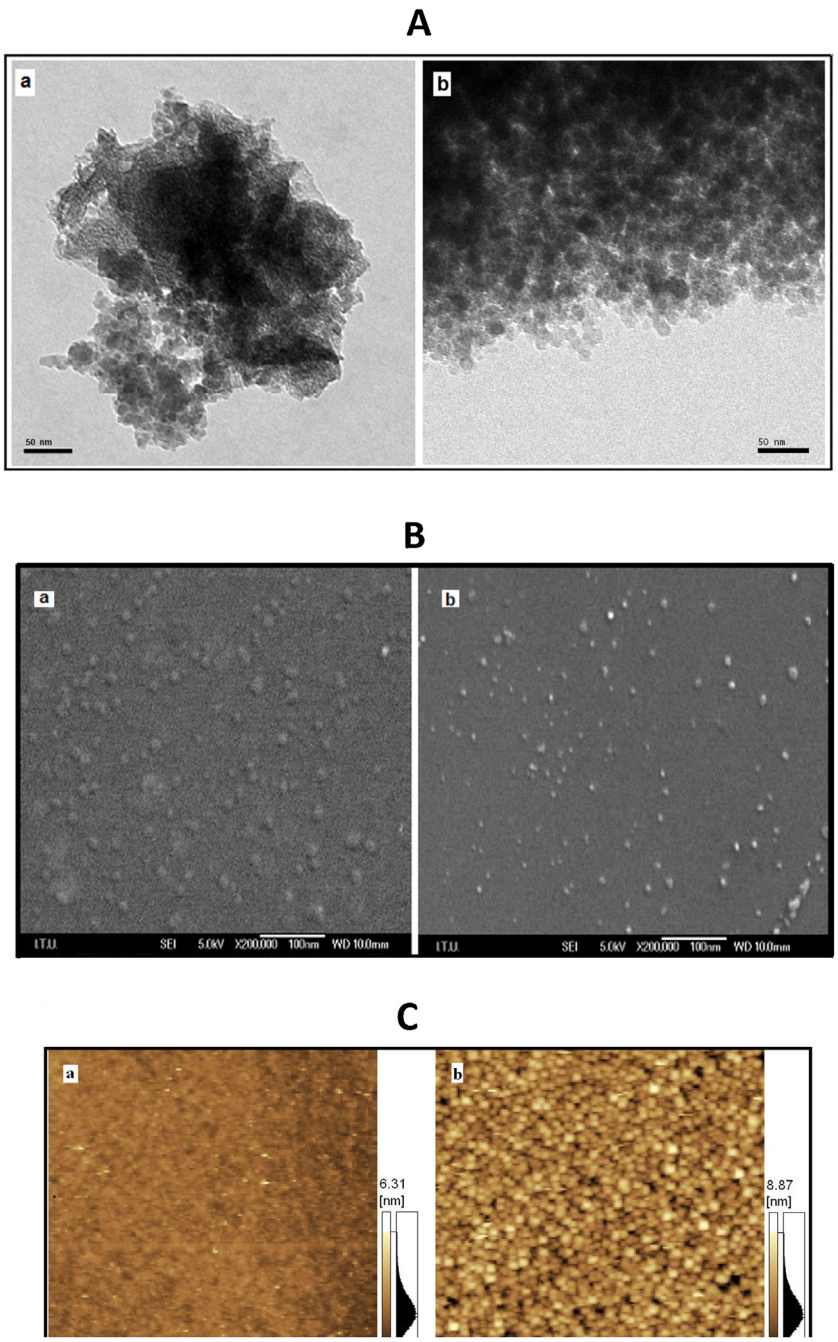


**Fig. 2.** (A) TEM, (B) SEM, (C) AFM images of AZO nano films with different ZnO:water ratios: (a) 5, (b) 2.5.

temperature. The increase in the heat treatment temperature encouraged the high crystallization, which led to the increase in the crystallite size of the AZO nano-composite films. The average crystallite sizes calculated from the XRD data of all films were summarized in Fig. 1D. The activation energy of AZO nano-composite films was determined by the Arrhenius equation as $E = -RT \ln(d/a)$ where $T$ is the temperature (Kelvin), $R$ is the universal gas constant, $d$ is the average crystallite size, and a is the intercept. The activation energy of AZO nano-composite films was calculated as 49 kJ/mol for the nanoparticles' growth using the slope of the lines of the plot in Fig. 1E.

The microstructure and morphology of AZO films were determined with TEM, SEM and AFM measurements. TEM images of AZO nano-composite films synthesized as ZnO:Al ratio %2 at 500 °C were shown for various ZnO:water ratios in Fig. 2A. The sizes of nanoparticles increased with the decreasing ZnO:water ratio.

SEM images of AZO films were presented in Fig. 2B. The surfaces of the films were observed as a uniform and nano-sized structure. The size of nano particles was decreased with the increase in the ZnO:water volume ratios. These results were promoted by XRD and TEM measurements. The surface roughness of AZO nano-composite films was observed for different ZnO:water volume ratios using AFM. AFM images of AZO films are showed in Fig. 2C. The roughness of AZO films was determined to be Rms: 2.96; 3.31; 4.04; 6.54 nm for 5; 4; 2.5; 2, ZnO:water ratios. The roughness of the films increased with a decrease in the ZnO:water ratio. The surface roughness of AZO films was determined to be Rms: 3.06; 4.19; 5.37; 6.81 nm for 4; 3; 2; 1% ZnO:Al ratios.

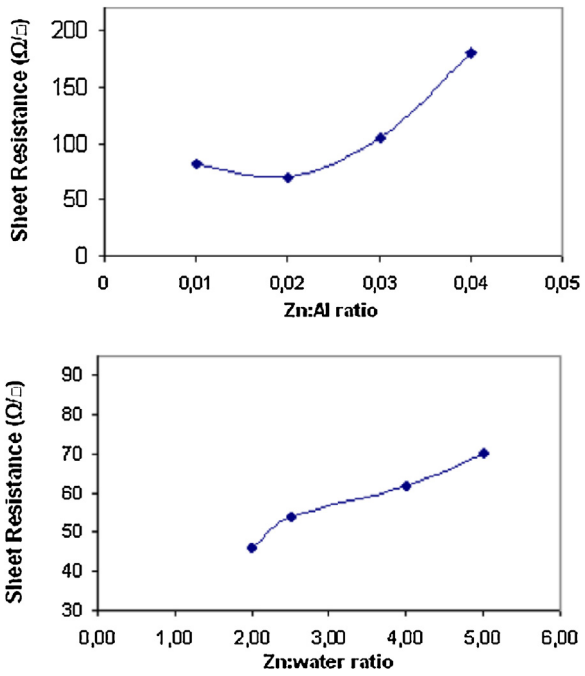


**Fig. 3.** Surface resistivity of AZO nano films for different ZnO:Al and ZnO:water ratios.

### 3.2. Electrical analysis

The sheet resistance of the AZO nano-composite films was measured by a four-point probe. When ZnO:water ratio was held fixed at 5, the surface resistivity of AZO film was measured for different ZnO:Al ratios as shown in Fig. 3. The electrical resistivity of the films decreased from 180 to 82 Ω/□ as the ZnO:Al ratio decreased from 4 to 1%. Additionally, when ZnO:Al ratio is fixed as 2%, the surface resistivity of AZO film was determined for different ZnO:water ratios in Fig. 3. The electrical resistivity of the films decreased from 70 to 46 Ω/□ as the ZnO:water ratio decreased to 2%.

However, the resistivity of the film ZnO:Al at 3% increased greatly to 115 Ω/□. ZnO:water and ZnO:Al ratios are very important parameters for the improvement of electrical conductivity mechanism of the AZO nano-composite films due to the generation of more donor levels. When Al was doped with ZnO, Al and ZnO atoms merge into the ZnO lattice, and then free charge carriers increase in AZO films. This result contributes to the conductivity that decreases the surface resistivity of AZO films. The results indicated that the large increase in conductivity was determined with the increment of ZnO:water ratio because of the adsorption of water. Al doping with 2% concentration is found to be the optimal ratio in terms of resistivity, and with above 3% Al doping concentration, the resistivity of AZO nano-composite films starts to increase.

### 3.3. Optical analysis

Absorbance values of AZO nano-composite films were measured using UV–vis spectrophotometer for different ZnO:Al and ZnO:water ratios in Fig. 4A and B. It clearly shows that the decreased in the ZnO:Al ratio produces a blue shift in the absorbance spectra of the films in Fig. 4A due to quantum size effect. The diffrence in the absorption edge is related to Burstein–Moss effect because of the increasing water in Fig. 4B [21,22]. Transmittance values of the films were decreased with the increasing ZnO:Al ratios in Fig. 4C. Additionally, transmittance of the films were decreased with the decreased ZnO:water ratios as shown in Fig. 4D.

The optical transmittance increased from 91 to about 93% by 1% and then decreased for 2% Al. The transmittance also increased up to 1% Al. With a further increase in the doped concentration, Al atoms occupy interstitial sites and increase the absorption. The optical band gap ($E_g$) of the AZO thin film was determined by the Tauc's relation [23]:

$$\alpha h\nu \propto \left(h\nu - E_g\right)^{1/2}$$

where the absorption coefficient ($\alpha$), optical band-gap energy ($E_g$), $h$ is the Plank's constant, $\nu$ is the frequency of the incident photon; for a direct transition as illustrated in Fig. 5. The effect of the ZnO:Al on AZO films increased the band gap values from 3.15 to 3.32 eV for 1 and 4% doped films. The band gap values of AZO nanocomposite films decrease after lowering ZnO:water ratio from 5 to 2, and ZnO:Al ratio at 2% is found to be 3.24–3.28 eV, respectively. The shift to a shorter wavelength in the absorption edge is

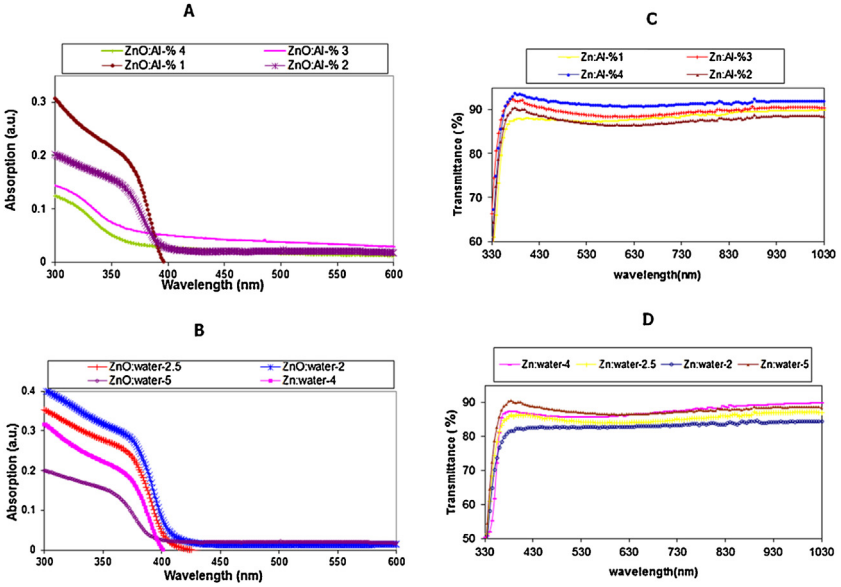


**Fig. 4.** (A) UV–vis absorption spectra of AZO nano films for different ZnO:Al ratios. (B) UV–vis absorption spectra of AZO nano films for different ZnO:water ratios. (C) Transmittance spectra of AZO nano films for different ZnO:Al ratios. (D) Transmittance spectra of AZO nano films for different ZnO:water ratios.

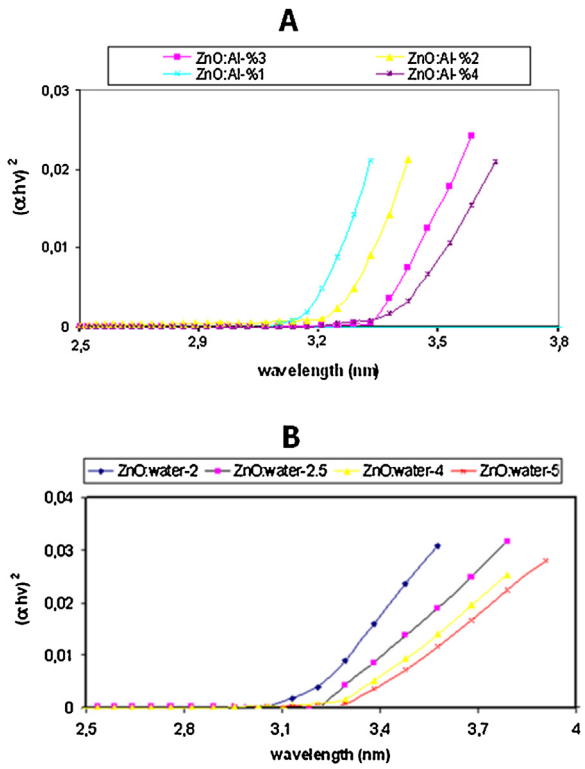


**Fig. 5.** $(\alpha h\nu)^2$–$h\nu$ graphs of AZO nano films for different (A) ZnO:Al ratios, (B) ZnO:water ratios.

associated with the Burstein–Moss effect due to Fermi level which enters into the conduction band. AZO films show absorption in the longer wavelength region by decreasing ZnO:water. Thus, the decrease in the band gap of films can contribute toward the electrical conductivity of the AZO films. Similar band gap energy calculation of ZnO:Al samples was also done before for the other transparent ZnO nanostructured thin films are deposited on the substrate, but using pulsed laser deposition (PLD) and spray pyrolysis techniques [24,25]. The band gap of films was reported to found in the range from 3.72 to 3.46 eV in these studies. Calculated band gap energy values of our sol–gel derived AZO nano-composite films are much lower in comparison to reported in other studies. This indicates that it is possible to alter transparency and conductivity of the films with varying the composition of the films.

## 4. Conclusions

In this study, we report on the preparation and structural characterization of AZO films. The structural, electrical and optical properties of AZO films were determined by changing ZnO:water and ZnO:Al volume ratio. This work has shown that AZO thin films are obtained as hexagonal wurzite structure at 500 °C heat treatment temperature. The crystallite size values are calculated for various ZnO:Al and ZnO:water ratios. The surface resistivity, the activation energy for the nanoparticles growth and the band gap values of AZO nano-composite films can be controlled by changing ZnO:water and ZnO:Al ratios. The results indicate that a decrease in the ZnO:water ratio leads to the increase in the crystallite size of AZO films due to the agglomeration. The roughness of AZO films also increases with the increasing crystallite size. AZO films exhibit absorption in the shorter wavelength region with the decreasing crystallite size, which consequently increases the band gap values of the films. The decrease in the ZnO:water ratio results in the increase in the crystallite size leading to the lower resistivity and higher conductivity due to the carriers. The film surface resistivity decreased from 180 to 82 Ω/□, and the average transmittance in the wavelength range of 330 and 1030 nm increased slightly from 87% to 93% for different ZnO:Al ratios. Additionally, when ZnO:Al ratio is fixed as 2%, the surface resistivity decreased from 70 to 46 Ω/□, and the average transmittance in the wavelength range of 330 and 1030 nm increased slightly from 82% to 91% for different ZnO:water ratios. Transmittance values of the films decrease with the decreasing ZnO:water ratio. The optimum values for surface resistivity and the optical transmittance of the films were determined to be 70 Ω/□ of resistivity and 86% of transmittance in visible region. As a result of this, AZO nano-composite films can be used easily in the electronic applications.

## Acknowledgments

The authors would like to thank Prof. Dr. Fatma Z. Tepehan (ITU Thin Film Laboratory). The Research Fund of Mimar Sinan University (BAP Project no: 201206) has generously supported this research.

## References

[1] M. Vishwasa, K. Narasimha Raob, A.R. Phani, K.V. Arjuna Gowdad, R.P.S. Chakradhar, Solid State Commun. 152 (2012) 324–327.
[2] M.H. Mamat, M.Z. Sahdan, Z. Khusaimi, A. Zain Ahmed, S. Abdullah, M. Rusop, Opt. Mater. 32 (2010) 696–699.
[3] C.G. Granqvist, Sol. Energy Mater. Sol. Cells 91 (2007) 1529–1598.
[4] S. Thanka Rajana, B. Subramaniana, A.K. Nanda Kumar, M. Jayachandrana, M.S. Ramachandra Rao, J. Alloys Compd. 584 (2014) 611–616.
[5] C.-Y. Tsay, K.-S. Fan, Y.-W. Wang, C.-J. Chang, Y.-K. Tseng, C.-K. Lin, Ceram. Int. 36 (2010) 1791–1795.
[6] Ü.Ö. Akkaya Arıer, B.Ö. Uysal, Mater. Sci. Semicond. Process. 24 (2014) 157–163.
[7] G. Srinivasan, R.T. Rajendra Kumar, J. Kumar, Opt. Mater. 30 (2007) 314–317.
[8] F.-H. Wang, H.-P. Chang, C.-C. Tseng, C.-C. Huang, H.-W. Liu, Curr. Appl. Phys. 11 (2011) 12–16.
[9] M.S. Kim, K.G. Yim, J.-S. Son, J.-Y. Leem, Bull. Korean Chem. Soc. 33 (4) (2012) 1235–1241.
[10] C.T. Fragoso, R. Battisti, C. Miranda, P.C. de Jesus, J. Mol. Catal. A: Chem. 301 (2009) 93–97.
[11] N. Menek, E. Eren, S. Topçu, Dyes Pigm. 68 (2006) 205–210.
[12] C.P. Huang, Y.F. Huang, H.P. Cheng, Y.H. Huang, Catal. Commun. 10 (2009) 561–566.
[13] N. Neves, A. Lagoa, J. Calado, A.M. Botelho do Rego, E. Fortunato, R. Martin, I. Ferreira, J. Eur. Ceram. Soc. (2014), accepted paper.
[14] K. Lin, P. Tsai, Mater. Sci. Eng., B 139 (2007) 81–87.
[15] M. Vishwas, K. Narasimha Rao, A.R. Phani, K.V. Arjuna Gowda, R.P.S. Chakradhar, Solid State Commun. 152 (2012) 324–327.
[16] P. Zhang, R.Y. Hong, Q. Chen, W.G. Feng, Powder Technol. 253 (2014) 360–367.
[17] R.K. Shukla, A. Srivastava, A. Srivastava, K.C. Dubey, J. Cryst. Growth 294 (2006) 427–431.
[18] Z. Pan, J. Luo, X. Tian, S. Wu, C. Chen, J. Deng, C. Xiao, G. Hu, Z. Wei, J. Alloys Compd. 583 (2014) 32–38.
[19] H. Karaagac, E. Yengel, M.S. Islam, J. Alloys Compd. 521 (2012) 155–162.
[20] B.D. Cullity, The Elements of X-Ray Diffraction, Addison-Wesley, Reading, MA, 1978, pp. 102.
[21] E. Burstein, Phys. Rev. 93 (1954) 632.
[22] A. Segura, J.A. Sans, D. Errandone, D. Martinez-Garcí, V. Fages, Appl. Phys. Lett. 88 (2006) 011910.
[23] J. Tauc, Mater. Res. Bull. 5 (1970) 721.
[24] M.Y. Zhang, G.J. Cheng, Appl. Phys. Lett. 99 (2011) 051904.
[25] K. Vijayalakshmin, K. Karthick, D. Gopalakrishna, Ceram. Int. 39 (2013) 4749–4756.